Asociación Argentina
de Mecánica Computacional

Mecánica Computacional Vol XXXI, págs. 1893-1907 (artículo completo)
Alberto Cardona, Paul H. Kohan, Ricardo D. Quinteros, Mario A. Storti (Eds.)
Salta, Argentina, 13-16 Noviembre 2012

NUMERICAL MODELING OF HYDRATION PROCESS AND TEMPERATURE EVOLUTION IN EARLY AGE CONCRETE

Antonio Caggiano[a,b,d], Marco Pepe[b], Eduard A.B. Koenders[c,e], Enzo Martinelli[b] and Guillermo J. Etse[d]

[a] *Laboratory of Materials and Structures, University of Buenos Aires, Ciudad Autonoma de Buenos Aires, Argentina, acaggiano@fi.uba.ar*

[b] *Department of Civil Engineering, University of Salerno, Fisciano, Salerno, Italy, emails: mapepe@unisa.it, e.martinelli@unisa.it, http://www.encore-fp7.unisa.it/*

[c] *Faculty of Engineering, Federal University of Rio de Janeiro, Brazil*

[d] *CONICET, National University of Tucuman, Argentina, getse@herrera.unt.edu.ar*

[e] *Microlab, Delft University of Technology, The Netherlands, e.a.b.koenders@tudelft.nl*

Keywords: Concrete Curing, Finite Differences, Finite Element Method, Heat Transfer, Hydration.

Abstract. Heat production induced by the hydration reaction and the resulting temperature evolution in the early phases of setting and hardening processes are critical phenomena, often leading to premature cracking of concrete members. However, the interest for simulating such phenomena is also related to the fundamental relationships between the nature of the main concrete components, such as aggregates and binders, and its mechanical properties. As a matter of principle, the actual efficiency of the concrete mix can be assessed by monitoring the hydration process and the latter can be directly related to the development of the relevant mechanical properties. This paper presents a numerical model for simulating the hydration process of cement and the resulting time evolution of temperature inside concrete. In general, boundary conditions ranging between isothermal and adiabatic situations can be considered. Then, the heat-flow generated throughout the hardening concrete specimen as a result of these general boundary conditions can be simulated by the proposed model with the aim to analyze its effect on the cement hydration process and the resulting concrete maturity. After the analytical formulation of the hydration and heat transfer problems, a consistent numerical solution based on the Finite Difference (FD) technique is developed. Then, the same constitutive relationships are considered within a general Finite Element (FE) procedure. The numerical results obtained through FD and FE solutions are compared with the experimental results obtained from two concrete mixes in both adiabatic and non-adiabatic conditions. The comparison between the two numerical predictions and the corresponding experimental results confirms the accuracy of the proposed model. The FD numerical solution can be easily implemented in a spreadsheet.

1 INTRODUCTION

As a matter of principle, the mechanical behavior of concrete can be predicted by modeling in detail the complex phenomena arising from the hydration reaction which develops during the setting and hardening phases and results in the heat flow often responsible of premature cracking (van Breugel, 1991). Particularly, the behavior of concretes elaborated with partial replacement of recycled aggregates (Caggiano et al., 2011) and alternative binders can be better understood through such models (Aitcin, 2007). By doing so, it will be possible to take into account the thermal boundary conditions as they occur during the chemical cementitious reaction process (Koenders, 1997). From this, the models offer a way to consider the relationship of such thermal mechanisms with the development of the associated materials properties such as compressive strength and elastic modulus (Lokhorst, 1999).

A fundamental approach that can be employed to analyze the early age behavior of concretes with (partial) replacements of binders or aggregates would be to go back to the basic analytical formulations for temperature development and hydration, and use this as input for the evaluation of the (prevailing) formulae for the development of the material properties (De Schutter and Taerwe, 1996). This approach gives an enormous insight into the dependency of the material properties towards the basic parameters that control the progress of the hydration process. In this way, the direct relation between the degree of hydration and the outcome of the formulae for the development of the material properties can be envisioned systematically (Lokhorst, 1999).

Temperature increments, in hardening concrete elements associated with the development of the material properties, are the result of the exothermal chemical reaction between water and the cementitious binder. The relevance of simulating the temperature field of hardening concrete has been known for many decades (van Breugel, 1991). Incremental thermo-mechanical model aimed at investigating the heat production and hardening processes from hydration phenomena are recently proposed in literature. Relevant contributions can be found in (Cervera et al., 2002; Hattel and Thorborg, 2003; Ortiz et al., 2005; Faria et al., 2006).

This paper deals with a theoretical formulation aimed at investigating the physical/chemical problem for the hydration phenomena of early age concrete. The basic analytical formulae for temperature development and hydration are outlined in section 2. The governing Partial Differential Equation (PDE) outlined in the same section is solved numerically through the Finite Difference (FD) approach. Formulae that characterize the development of the material properties, such as the compressive strength and the elastic modulus, are also reported in the same section and can be used to assess the mechanical performance of concrete at different ages.

A numerical solution based on the Finite Element (FE) technique is developed in section 3. The basic equations studying the heat of hydration during the hardening process and the iterative integration scheme are reported therein. The results derived from the theoretical solutions and both numerical solutions (FD and FE, respectively) are validated against measurements achieved from experimental tests as proposed in section 4.

2 THEORETICAL FORMULATION

This section describes the main physical phenomena that occur during the concrete setting and hardening processes and outlines the key theoretical assumptions used to simulate the effects of concrete curing.

The main aspects are related to the liberation of heat due to the exothermic nature of the cement hydration reaction. The heat-flow, generated throughout the hardening concrete spec-

imen as a result of non-adiabatic boundary conditions, is analyzed to simulate the effect of variable temperature on the cement hydration process and the resulting concrete maturity. The relationships between the hydration process and the progressive development of the relevant mechanical properties of concrete are documented in this section.

2.1 Models for cement hydration

Modeling the hydration process of cementitious materials can be done in different ways (Jennings and Bullard, 2011). Plenty of theoretical proposals mainly concern the way in which the kinetics is addressed and the scale level at which the hydration processes are schematized (Dolado and van Breugel, 2011). Analytical models generally include the kinetics as a rate factor that changes throughout the progress of the hydration process, following a predefined mathematical function (Dabic et al., 2000; van Breugel, 1991).

Other more advanced computer-based models deal with describing the hydration process at a much higher level of detail, i.e. often at the micro-scale level. Even more details can be added when including richer reaction information, obtained from more accurate nano-scale level (Bullard et al., 2011). In general these classes of models use an integrated kinetics approach where the models describe the formation of interparticle contacts and their explicitly effect on the reaction rate (Bentz et al., 1993). This approach, in general, explicitly simulates the cement chemistry, the particle size distribution, the water to cement ratio and the temperature. With these models, the degree of hydration, representing the amount of cement that has actually reacted with water, can be quantified.

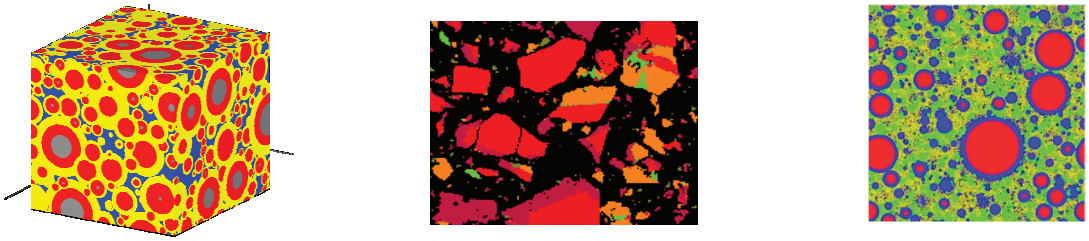

(a). Hymostruc (b). CEMHYD3D (c). µic

Figure 1: Impression of three advanced hydration models that operate at the micro-scale level: (a) Hymostruc (van Breugel, 1991), (b) CEMHYD3D by Bentz et al. (1993) and (c) μic by Bischnoi (2008).

However, as it can be observed from the 3D schematizations presented in Fig. 1, modeling but also measuring the degree of hydration experimentally is a complex and very demanding exercise. In the proposed model the degree of hydration is calculated from the actual amount of heat relative to the total amount of heat that liberates after full hydration of all the cement in the system. However, in general, instead of the liberated heat, the adiabatic temperature curve is used to characterize the hydration process. The actual state of hydration in the system is then characterized by the quotient of the actual temperature and the maximum adiabatic temperature, and this multiplied by the maximum degree of hydration that will potentially be reached after hydration has ceased. This makes it possible to use the adiabatic temperature curve as model input and to avoid complicated chemically-based hydration tests.

2.2 Adiabatic curing of concrete and degree of hydration

The chemical reactions, which take place during concrete setting and hardening, are mainly driven by the hydration process of cement grains within the concrete mix. The hydration reaction of cement is exothermic in nature and results in a significant production of heat inside the hardening concrete. The actual status of the cement reaction can be described by introducing the so-called *degree of hydration* $\alpha_h(t)$ which is defined as the ratio between the amount of hydrated cement at the time t and the total amount of cement within the mix (van Breugel, 1991; Ulm and Coussy, 1995).

Since the amount of hydrated cement at time t is proportional to the total amount of heat $Q(t)$ produced at the same time, the degree of hydration can be analytically defined as follows (De Schutter and Taerwe, 1995)

$$\alpha_h(t) = \frac{Q(t)}{Q_{\max}}, \tag{1}$$

where $Q_{\max}$ is the amount of heat liberated at the end of the hydration process.

The heat produced by the hydration reaction is significantly influenced by the temperature which depends on the sample dimensions, boundary conditions and, therefore, is also controlled by the produced heat itself. Particularly, a simple analytical relationship can be written between the degree of hydration α_h and the corresponding variation of the adiabatic temperature increment $\Delta T_a(t)$, in the ideal case of adiabatic conditions

$$\Delta T_a(t) = \frac{C Q_{\max}}{\rho_c c_c} \alpha_h(t) \tag{2}$$

where C is the cement content per unit volume, ρ_c the specific mass of concrete and c_c the specific heat of concrete.

Thus, the current temperature $T_a(t)$ developed within the hardening concrete can be expressed by introducing in Eq. (2) the definition of α_h reported in Eq. (1)

$$T_a(t) = T_R + \Delta T_a(t) = T_R + \frac{C}{\rho_c c_c} Q_a(t) \tag{3}$$

where Q_a is the amount of heat liberated in adiabatic condition, T_R the room temperature and then, in such conditions the degree of hydration (consistently denoted as $\alpha_{a,h}$) can also be expressed in terms of temperature increase

$$\alpha_{a,h}(t) = \frac{Q_a(t)}{Q_{\max}} = \frac{\Delta T_a(t)}{\Delta T_{a,\max}} \alpha_{h,\max} \tag{4}$$

where $\alpha_{h,\max}$ is the degree of hydration theoretically achieved at the end of the hydration process (namely, in the limit for $t \to \infty$).

Based on the experimental results on hardening concrete samples in adiabatic conditions, van Breugel (1991) proposed two possible analytical expressions to approximate the observed time evolution of heat $Q_a(t)$

$$Q_a(t) = Q^*_{\max}\left(1 - e^{-rt}\right) \tag{5}$$

$$Q_a(t) = Q^*_{\max} e^{-\left(\frac{\tau}{t}\right)^{\beta}} \tag{6}$$

where $Q^*_{\max}$ is the total heat produced by the hydration reaction in adiabatic conditions; r, τ and β control the shape of the functions introduced to describe the heat evolution in the time

t. Further details about the above mentioned parameters can be found in Pepe et al. (2012) and Martinelli et al. (2012).

As a matter of principle, the following relationship can be stated between $Q^*_{\max}$ and $Q_{\max}$

$$Q^*_{\max} = Q_{\max}\left[\lim_{t\to\infty} \alpha_h\left(t\right)\right] = Q_{\max}\alpha_{h,\max}. \tag{7}$$

For the sake of simplicity, the following developments presented in this paper will be based upon the assumption of the relationship reported in Eq. (5).

2.3 Heat production and flow in concrete during setting and hardening

Since concrete is generally cured under non-adiabatic conditions, heat-flow occurs throughout the concrete body during setting and hardening and results in a transient temperature field.

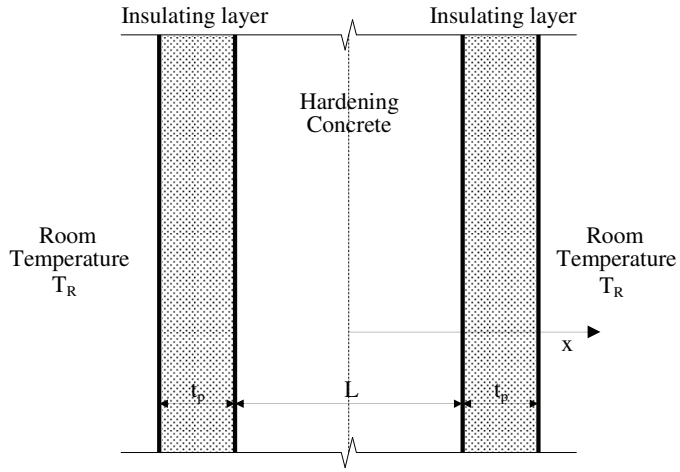

Figure 2: Geometrical description of the 1D problem.

As a matter of principle, the non-stationary heat conduction problem, characterizing the thermal behavior of concrete during setting and hardening, can be described by the well-known Fourier equation (Narasimhan, 1999). In the case of the 1D geometry considered in the present study (Fig. 2), such a PDE takes the following analytical expression

$$\rho_c c_c \frac{\partial T}{\partial t} = \lambda_c \frac{\partial^2 T}{\partial x^2} + q_c(x,t) \tag{8}$$

where λ_c is the heat conduction coefficient, T is the temperature field in concrete, t the time and

$$q_c\left(x,t\right) = C\frac{dQ_c}{dt} \tag{9}$$

is the rate of heat source where Q_c is the function describing the heat produced by the hydration reaction of cement in general (non-adiabatic) conditions.

As already mentioned in section 2.2, heat source q_c is significantly affected by the actual values of temperature developed inside the concrete sample. Then, since temperature itself depends on the produced heat, a clear feedback effect can be recognized between q_c and T. The effect of absolute temperature T on the rate $V(T)$ of chemical reaction can be generally

expressed through the well-known *Arrhenius equation* which can be analytically described by the following relationship (Acker, 1988)

$$V\left(T\right) = A_V e^{-\frac{E_A}{RT}} \tag{10}$$

where A_V is a reference rate value, E_A is the activation energy (usually expressed in J/mol) and R is the universal gas constant ($R \approx 8.3145\, J/molK$). In principle, the values of A_V and E_A can be determined by measuring the rate V under two different temperature values. However, the following applications will be based on assuming $E_A = 33000\, J/mol$ for hardening concrete, according to experimental results currently available in the scientific literature (van Breugel, 2004; Kada-Benameur et al., 2000; D'Aloia and Chanvillard, 2002).

The Arrhenius equation (10) is useful to express the relationship between the actual rate of flow $q_c(T)$ and the corresponding $q_a(T_a)$ which should have been measured under adiabatic conditions at the same stage of the hydration reaction. Thus, if the semi-adiabatic process has achieved the degree of hydration $\alpha_h(t)$ at the time t, an equivalent time t_{eq} can be defined to identify the corresponding status of the hydration reaction under adiabatic conditions

$$Q_a\left(t_{eq}\right) = \alpha_h\left(t\right) Q_{\max} \tag{11}$$

The actual analytical expression of t_{eq} depends on the analytical form chosen for describing the function $Q_a(t_{eq})$. For instance the following two expressions correspond to the two functions reported in Eqs. (5) and (6), respectively

$$\left(1 - e^{-rt_{eq}}\right) = \frac{\alpha_h\left(t\right)}{\alpha_{h,\max}} \qquad \Longrightarrow \qquad t_{eq} = -\frac{1}{r}\ln\left[1 - \frac{\alpha_h\left(t\right)}{\alpha_{h,\max}}\right] \tag{12}$$

and

$$e^{-\left(\frac{\tau}{t_{eq}}\right)^{\beta}} = \frac{\alpha_h\left(t\right)}{\alpha_{h,\max}} \qquad \Longrightarrow \qquad t_{eq} = -\frac{\tau}{\left\{\ln\left[\frac{\alpha_h(t)}{\alpha_{h,\max}}\right]\right\}^{\frac{1}{\beta}}} \tag{13}$$

Although, in principle, the amount of heat $Q_c(T)$ produced by the general hydration process is equal to that correspondingly generated in the ideal process up to the time t_{eq}, the two temperatures T and T_a developed in the two systems at time t and t_{eq} are not equal, as a result of the heat transfer phenomena taking place in the former. Having pointed out this aspect, a clear relationship can be stated through Eq. (10) between the rate of the heat source in the two above mentioned conditions

$$\frac{q_c\left[T\left(t\right)\right]}{q_a\left[T_a\left(t_{eq}\right)\right]} = \frac{e^{-\frac{E_A}{RT(t)}}}{e^{-\frac{E_A}{RT_a(t_{eq})}}} = e^{-\frac{E_A}{R}\frac{T_a(t_{eq})-T(t)}{T_a(t_{eq})T(t)}}. \tag{14}$$

As clearly demonstrated in De Schutter and Taerwe (1996), the above approach is more accurate for concrete whose binder is mainly made of Portland Cement (e.g., CEM I and CEM II according to the European Classification EN-197-1 (2011)), as a unique dominant reaction phase can be recognized in such materials. Under this limitation, the following analytical expression can be determined for the PDE describing the heat flow in hardening concrete

$$\rho_c c_c \frac{\partial T}{\partial t} = \lambda_c \frac{\partial^2 T}{\partial x^2} + q_a\left[T_a\left(t_{eq}\right)\right] e^{-\frac{E_A}{R}\frac{T_a(t_{eq})-T(t)}{T_a(t_{eq})T(t()))}} \tag{15}$$

where the flow source in adiabatic conditions can be determined as follows

$$q_a\left[T_a\left(t_{eq}\right)\right] = C\frac{dQ_a}{dt}\bigg|_{t=t_{eq}}. \tag{16}$$

Equation (15) can be solved numerically. However, initial and boundary conditions are also needed for its space-time integration.

Initial Dirichlet conditions are rather simple, as room temperature T_R has to be imposed to all the space domain at $t = 0$

$$T\left(x, t=0\right) = T_R. \tag{17}$$

Boundary conditions at the two external sides can be directly imposed if the time evolutions $T_{left}(t)$ and $T_{right}(t)$ of temperature, measured there during the hydration process, are actually available

$$\begin{array}{l} T\left(x=-L/2, t\right) = T_{left}\left(t\right) \\ T\left(x=L/2, t\right) = T_{right}\left(t\right) \end{array} \tag{18}$$

More often an insulating layer bounds the two external faces of the concrete specimen. If t_p is the thickness of such a layer, and λ_p is its heat conduction coefficient, the boundary conditions can be derived by expressing the continuity of the heat flow throughout the insulation-concrete interfaces

$$q_{left}\left(t\right) = \lambda_p\frac{T_{left}(t) - T_R}{t_p} = \lambda_c\frac{\partial T}{\partial x}\bigg|_{x=-L/2}, \tag{19}$$

$$q_{right}\left(t\right) = \lambda_p\frac{T_{right}(t) - T_R}{t_p} = -\lambda_c\frac{\partial T}{\partial x}\bigg|_{x=L/2}. \tag{20}$$

Thus, equation (15), initial conditions (17) and boundary ones (19) and (20), completely describes the 1D heat-flow occurring within hardening concrete described in Figure 2.

3 FE MODELING OF HYDRATION AND HEAT TRANSFER IN HARDENING CONCRETE

The calculation of temperature and stress distributions of concrete mass during its hardening stage is of key importance in terms of crack control and durability performance of a considered concrete structure.

The analyses of heat of hydration, during the hardening process of concrete in a general 3D space, is proposed in this section. The thermal behavior is carried out by using a 3D finite element approach. The theoretical model presented in section 2 is accounted into the commercial FE code Midas/FEA (Midas-IT-User-Manual, 2010) with the aim to investigate the hydration and heat transfer of the considered concrete samples.

3.1 Basic equations

As proposed in section 2.3, the non-stationary heat conduction problem in a general three-dimensional space, can be described by the following Fourier equation

$$\rho_c c_c\frac{\partial T}{\partial t} - \nabla\cdot\left(k\,\nabla\left(T\right)\right) = q_c(T) \tag{21}$$

being k the thermal conductivity, while $\nabla\cdot$ and ∇ represent the divergence and the gradient operators, respectively (herein $\nabla^2[] = \nabla\cdot\nabla[]$ is the Laplace operator).

The temperature field T is discretized in the Finite Element (FE) domain assuming the following interpolation strategy

$$T = \mathbf{N} \cdot \hat{\mathbf{T}} \quad \rightarrow \quad \nabla T = \nabla \mathbf{N} \cdot \hat{\mathbf{T}} \tag{22}$$

where $\mathbf{N} = [h_1, h_2, ..., h_n]^t$ is the vector collecting the shape functions, while $\hat{\mathbf{T}} = [\hat{T}_1, \hat{T}_2, ..., \hat{T}_n]^t$ the nodal temperatures of the iso-parametric FE having n nodes. The first derivative with respect to time t of Eq. (22) can be expressed as follows

$$\frac{dT}{dt} = \mathbf{N} \cdot \frac{d\hat{\mathbf{T}}}{dt} = \mathbf{N} \cdot \dot{\hat{\mathbf{T}}} \tag{23}$$

The following equilibrium equation in the FE domain is used to analyze the heat transfer problem:

$$\mathbf{C^e} \cdot \dot{\hat{\mathbf{T}}} + \mathbf{K^e} \cdot \hat{\mathbf{T}} = \mathbf{F^e_Q} + \mathbf{F^e_q} \tag{24}$$

being

$$\begin{aligned}
\mathbf{C^e} &= \int_\Omega \mathbf{N}^t \rho_c c_c \mathbf{N} \, d\Omega && \text{Capacity operator} \\
\mathbf{K^e} &= \int_\Omega \nabla \mathbf{N}^t k \nabla \mathbf{N} \, d\Omega && \text{Conductivity operator} \\
\mathbf{F^e_Q} &= \int_\Omega \mathbf{N}^t Q_v \, d\Omega && \text{Heat load due to heat source} \\
\mathbf{F^e_q} &= \int_{\Gamma_n} \mathbf{N}^t q_n \, d\Gamma_n && \text{Heat load due to heat flow}
\end{aligned}$$

where Q_v is the rate of heat source and q_n the heat flow, while the boundary surface of the considered FE is denoted by Γ_n (in which the natural or Neumann conditions are imposed) having a volume Ω.

By using the classical assembling procedures for the FE analyses in structural problems, the following set of equations can be obtained

$$\mathbf{C} \cdot \dot{\mathbf{T}} + \mathbf{K} \cdot \mathbf{T} = \mathbf{F_Q} + \mathbf{F_q} \tag{25}$$

being $\mathbf{C}$ and $\mathbf{K}$ global constitutive matrices while $\mathbf{F_Q}$ and $\mathbf{F_q}$ the assembled global vectors. $\mathbf{T}$ is the vector of the nodal temperatures on the global reference system.

3.2 Integration method

In this section the well-known $alpha$-method is outlined as numerical approach for integrating stage-by-stage the evolution in time of Eq. (25). The following assumption is introduced in the time domain:

$$\alpha \dot{\mathbf{T}}_{t+\Delta t} + (1-\alpha)\dot{\mathbf{T}}_t = \frac{\mathbf{T}_{t+\Delta t} - \mathbf{T}_t}{\Delta t} \tag{26}$$

Then, the following relationship can be achieved by evaluating and joining the equilibrium equation (26), at time t and $t + \Delta t$,

$$\mathbf{C} \cdot \left(\alpha \dot{\mathbf{T}}_{t+\Delta t} + (1-\alpha)\dot{\mathbf{T}}_t \right) + \mathbf{K} \cdot (\alpha \mathbf{T}_{t+\Delta t} + (1-\alpha)\mathbf{T}_t) = \alpha \mathbf{R}_{t+\Delta t} + (1-\alpha)\mathbf{R}_t \tag{27}$$

being $\mathbf{R} = \mathbf{F_q}$.

Then, by introducing Eq. (26) into Eq. (27), the following equilibrium equation as a function of nodal temperatures can be obtained

$$(\mathbf{C} + \alpha \Delta t \mathbf{K}) \cdot \mathbf{T}_{t+\Delta t} = (\mathbf{C} - (1-\alpha)\Delta t \mathbf{K}) \cdot \mathbf{T}_t + \Delta t \left(\alpha \mathbf{R}_{t+\Delta t} + (1-\alpha)\mathbf{R}_t \right) \tag{28}$$

in compact form

$$\bar{\mathbf{K}} \cdot \mathbf{T}_{t+\Delta t} = \bar{\mathbf{R}} \tag{29}$$

being

$$\bar{\mathbf{K}} = \mathbf{C} + \alpha \Delta t \mathbf{K}$$
$$\bar{\mathbf{R}} = (\mathbf{C} - (1-\alpha)\Delta t \mathbf{K}) \cdot \mathbf{T}_t + \Delta t \left(\alpha \mathbf{R}_{t+\Delta t} + (1-\alpha)\mathbf{R}_t\right)$$

The value of the variable α adopted in this papers is $\alpha = 1$ dealing with a Backward-Euler method characterized by unconditional convergence.

4 APPLICATIONS AND COMPARISONS

In this section several numerical analyses are performed with the aim to validate the numerical proposals against the hydration process and the heat transfer behavior of early age concretes tested in both adiabatic and non-adiabatic conditions.

4.1 Experimental benchmark

The model presented in section 2 needs to be validated in its capability for simulating the hydration process under both adiabatic and non-adiabatic conditions. The hydration process of four concrete mixtures, characterized by a water-cement ratio $w/c = 0.4$ was observed at the Delft University of Technology (The Netherlands) and reported in Koenders (2005). However, since the model for hydration heat mentioned in subsection 2.3 can be exclusively applied to Portland Cement based concretes, only the specimens denoted as "Mixture 3" and "Mixture 4" are considered in the present study. Particularly, Mixture 3 is made of $450\ kg/m^3$ of CEM I 32.5 and the addition of 5% of silica-fume, whereas only $450\ kg/m^3$ of CEM II/A was employed in Mixture 4.

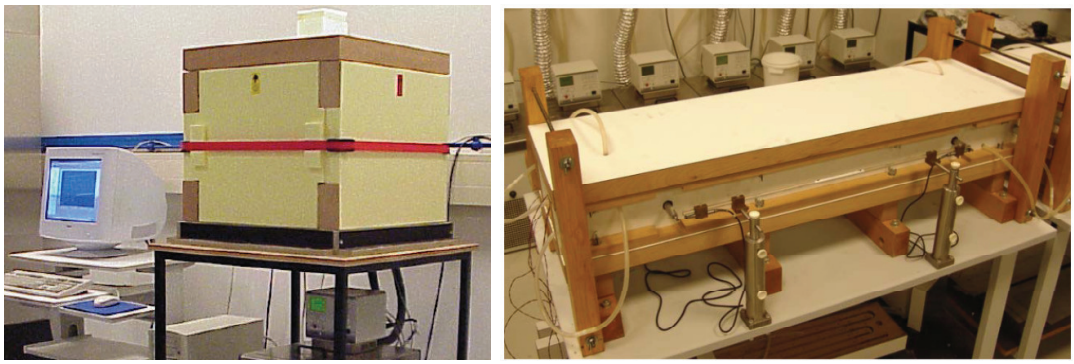

a) Adiabatic conditions *b) Non-adiabatic conditions*

Figure 3: Experimental equipments by Koenders (2005).

The adiabatic hydration curve is measured from a freshly cast concrete cube for which the thermal boundary conditions are controlled in such a way that heat liberation to the surrounding is prevented. This means that all heat that is generated inside the concrete cube will be used in favor of the rate of the chemical reaction process. It is a method to calculate the maximum heat generated by the concrete. The test set-up to determine the adiabatic hydration curve consists of an insulated mold of which the thermal boundary conditions are controlled by computer and a cryostat unit (Fig. 3a).

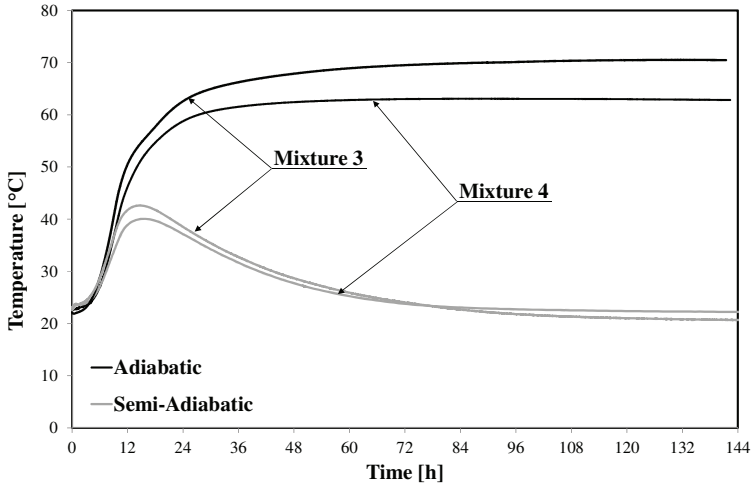

Figure 4: Experimental results: time evolution of temperature by Koenders (2005).

To measure the semi-adiabatic temperature evolution a dummy setup is used (Fig. 3b), which is part of the Thermal Stress Testing Machine (TSTM). This setup is generally used to measure the temperature development and free deformations of hardening concrete. The temperature evolution is measured in the centre of the specimen, at half the specimen height; the thickness of the specimen is $100\ mm$, the width $150\ mm$ and the length $750\ mm$, as shown in Fig. 3b. The mold is thermally insulated which leads to the increased temperature evolution during hardening (semi-adiabatic).

Figure 4 describes the time evolution of temperatures measured in the specimens made of the Mixtures 3 and 4 in the conditions described above. As expected, monotonic behavior was observed for both mixtures in adiabatic conditions, whereas significantly lower maximum temperatures develop in semi-adiabatic conditions as a results of the heat flow.

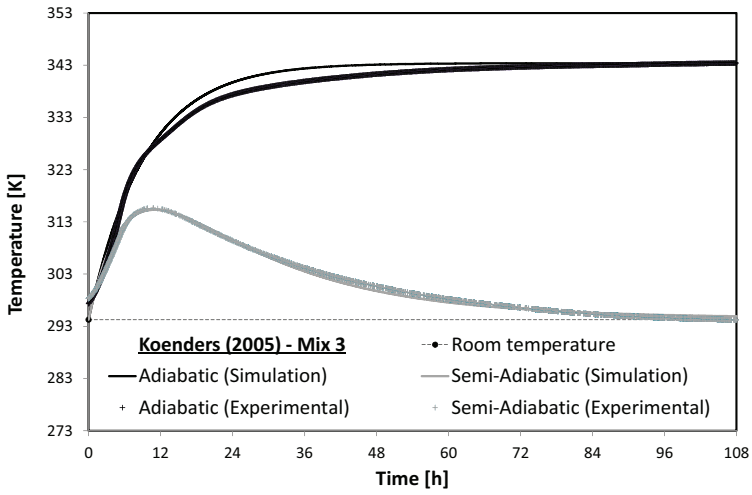

Figure 5: Comparison between the experimental data by Koenders (2005) and the theoretical results of the time evolution of Temperature (adiabatic heat production according to Eq. (5)): Mixture 3.

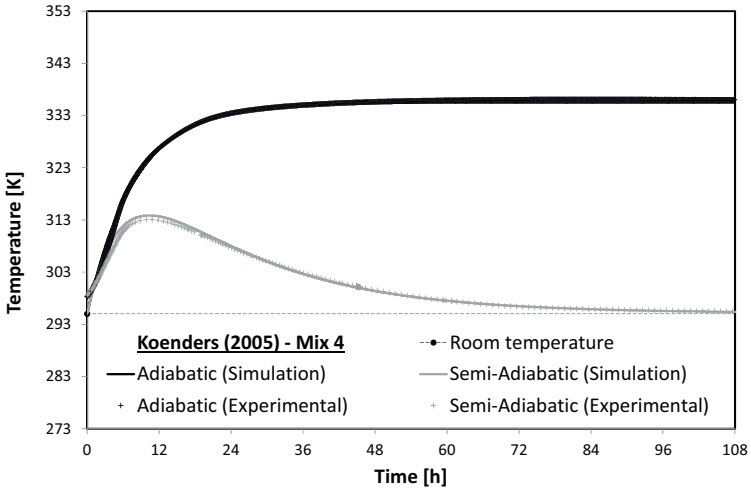

Figure 6: Comparison between the experimental data by Koenders (2005) and the theoretical results of the time evolution of Temperature (adiabatic heat production according to Eq. (5)): Mixture 4.

4.2 One-dimensional Hydration prediction

This subsection deals with the numerical results obtained through the 1D analytical formulation of the hydration and heat transfer problem given in subsection 2.3 and solved by means the application of a (FD) technique. Particularly the one-dimensional scheme proposed in Fig. 2 is here considered.

Figures 5 and 6 give both the adiabatic and non-adiabatic temperature histories obtained for the Portland Cement based concretes using the test equipment outlined in section 4.1. Assuming a specific heat, multiplied by the specific mass of concrete, $\rho_c c_c = 2500\ kJ/m^3K$, the temperature curves can be simulated by means of the hydration model outlined in section 2 with the 1D assumption proposed in subsection 2.3.

The thermal parameters employed in the numerical evaluations are: the heat conduction coefficient of concrete $\lambda_c = 2.5\ W/mK$, the activation energy of the Arrhenius function $E_A = 33000\ J/mol$, the universal gas constant $R = 8.31\ J/molK$ and the room temperature $T_R = 295\ K$. On the other hand, the parameters calibrated for the two concrete, above mentioned, are listed as follows:

- CEM I 32.5: $\alpha_{h,max} = 0.78$, $Q_{max} = 350\ kJ/kg$ and $r = 0.000030\ s^{-1}$.
- CEM II/A: $\alpha_{h,max} = 0.75$, $Q_{max} = 300\ kJ/kg$ and $r = 0.000035\ s^{-1}$.

The numerical predictions, in terms of Temperature vs. Time proposed in Figs. 5 and 6 and compared against experimental results, demonstrate a very good agreement. Actually, the proposed model is able to realistically reproduce the hydration process and the resulting temperature evolution in the early phases of setting and hardening of the considered concretes.

4.3 Three-dimensional FEM hydration analyses

This section describes the 3D FE simulation of the experimental tests reported by Koenders (2005) and already employed in subsection 4.2. The results in terms of temperature evolution in both adiabatic and non adiabatic test conditions at early ages is here reported.

Figure 7 shows the 3D geometry and the corresponding structural FE discretization employed in the present analysis by using regular hexahedral elements (with quadratic shape functions).

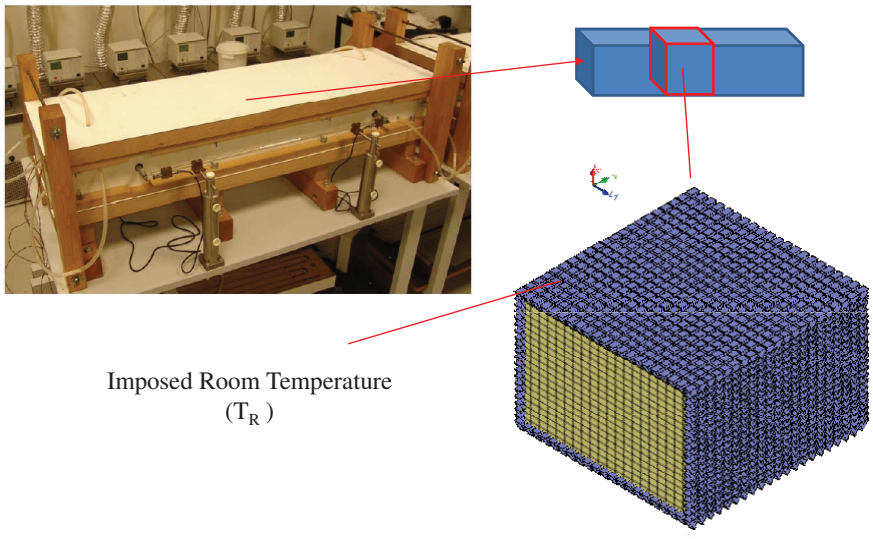

Figure 7: Geometry and boundary conditions of the FEM problem according to Koenders (2005) tests.

The front nodes and the opposites one of Fig. 7, where both convection conditions and constant temperatures are not specified, are analyzed under the adiabatic condition without any heat transfer. The simulation of a $150 \times 100 \times 150\ mm^3$ (base $\times$ height $\times$ length) concrete specimen, ideally extracted from the tested beams according to Koenders (2005) tests, is performed in this section. The same thermal parameters outlined in subsection 4.2 are considered.

Figs. 8 and 9 report the comparison between the temperature evolutions predicted by the FE modeling against the ones measured during the experimental tests, for the two different concretes. The calculated temperatures after different curing times can be shown in Figs. 10 and 11. Iso-thermal maps is generated by means of a contour plot from values defined at each considered time.

The overall agreement of the aging model predictions with the test results is fairly good and confirm the capability of the theoretical proposal for analyzing hydration and heat transfer problems.

5 CONCLUDING REMARKS

A model aimed at characterizing the hydration phenomenon of early stage concretes is proposed in this work. It emphasizes the role of hydration degree to describe the evolution of the hardening process. After the analytical formulation of the hydration and heat transfer problems, a consistent numerical solution based on the Finite Difference (FD) technique for 1D analyses is developed. Then, in order to consider structural applications dealing with the thermal problems, the same constitutive relationships are considered within a general Finite Element (FE) procedure. Numerical comparisons with experimental tests performed for Portland cement based concretes demonstrate the soundness and capability of the given proposal.

The method presented in this article shows a consistent and fundamental approach to investigate the physical/chemical problem for the hydration and aging phenomena of concrete curing.

Further developments are currently ongoing to assess the heat transfer and curing aspect

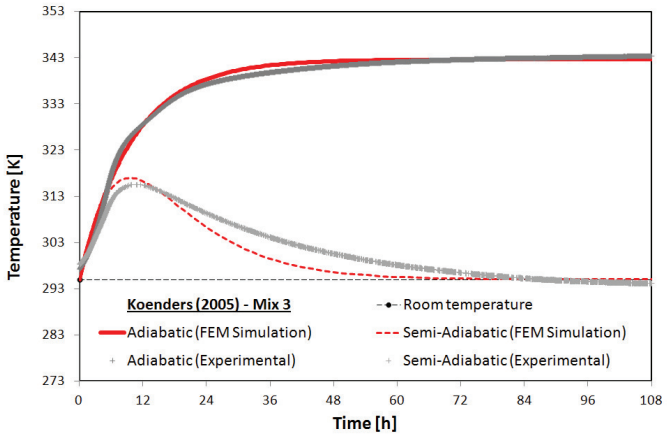

Figure 8: Comparison between the experimental data by Koenders (2005) and the FEM based results (adiabatic heat production according to Eq. (5)): Mixture 3.

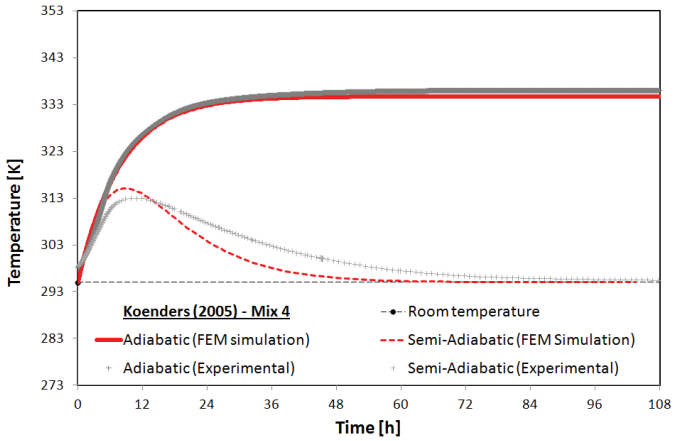

Figure 9: Comparison between the experimental data by Koenders (2005) and the FEM based results (adiabatic heat production according to Eq. (5)): Mixture 4.

of recycled aggregate concretes. Test results in this topic are recently determined within the framework of the European EnCoRe project www.encore-fp7.unisa.it.

ACKNOWLEDGMENTS

The support to networking activities provided by "Encore" Project (FP7-PEOPLE-2011-IRSES n 295283; http://www.encore-fp7.unisa.it/) funded by the European Union within the Seventh Framework Programme is gratefully acknowledged by the authors. The first and fourth authors also gratefully acknowledge the CSP Fea s.c. for the support in the FEM analyses.

REFERENCES

Acker P. *Comportement mecanique du beton: apports de l'approche physico-chimique*. In: Rapport de recherche N. 152. Paris: Laboratoire Ponts et Chaussees, 1988.

Aitcin P. *Binders for Durable and Sustainable Concrete (Modern Concrete Technology)*. CRC Press, 2007.

Bentz D., Garboczi E., and Stutzman P. *Computer Modelling of the Interfacial Transition Zone in Concrete*. in Interfaces in Cementitious Composites, edited by J.C. Maso (E. and F.N. Spon, London), pp. 259-268, 1993.

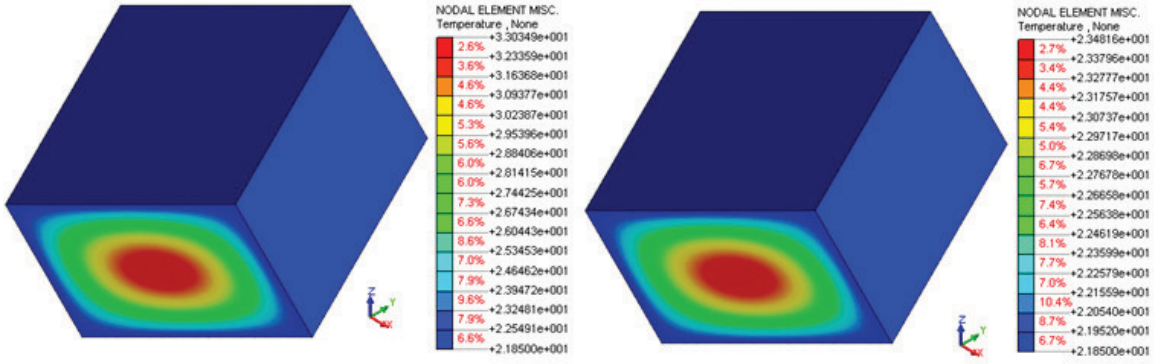

(a) (b)

Figure 10: Temperature evolutions $[°C]$ of the Mixture 3 in non-adiabatic condition: (a) after 24 h and (b) after 48 h.

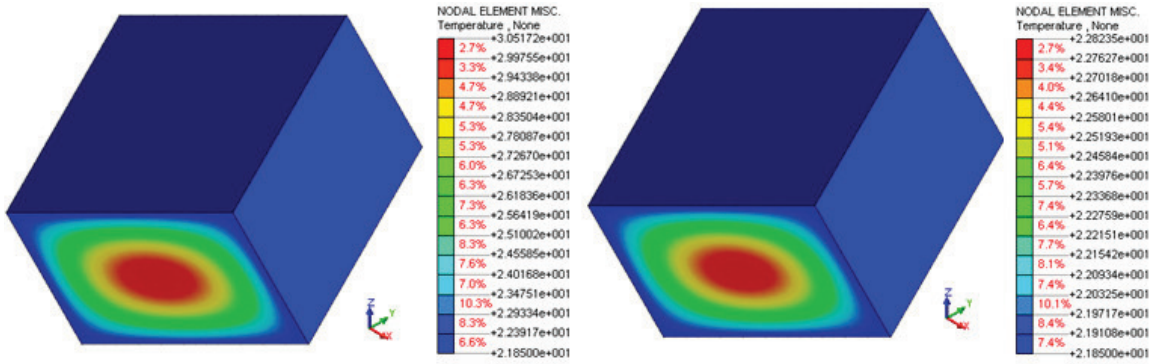

(a) (b)

Figure 11: Temperature evolutions $[°C]$ of the Mixture 4 in non-adiabatic condition: (a) after 24 h and (b) after 48 h.

Bischnoi S. *Vector Modelling of Hydrating Cement Microstructure and Kinetics*. PhD thesis, EPFL, Switzerland, 2008.

Bullard J., Lothenbach B., Stutzman P., and Snyder K. Coupling thermodynamics and digital image models to simulate hydration and microstructure development of portland cement pastes. *Journal of Materials Res*, 26:609 – 622, 2011.

Caggiano A., Faella C., Lima C., Martinelli E., Mele M., Pasqualini A., Realfonzo R., and Valente M. *Mechanical behavior of concrete with recycled aggregate*. 2nd Workshop on "The new boundaries of structural concrete" - ACI Italy Chapter, Ancona (Italy), 18-16 Settembre 2011, 55 - 62., 2011.

Cervera M., Faria R., Oliver J., and Prato T. Numerical modelling of concrete curing, regarding hydration and temperature phenomena. *Computers & Structures*, 80(18 - 19):1511 – 1521, 2002.

Dabic P., Krstulovic R., and Rusic D. A new approach in mathematical modelling of cement hydration development. *Cement and Concrete Res*, 30(7):1017 – 1021, 2000.

D'Aloia L. and Chanvillard G. Determining the apparent activation energy of concrete: Ea-numerical simulations of the heat of hydration of cement. *Cement and Concrete Research*, 32(8):1277 – 1289, 2002.

De Schutter G. and Taerwe L. General hydration model for portland cement and blast furnace slag cement. *Cement Concrete Res*, 25(3):593 – 604, 1995.

De Schutter G. and Taerwe L. Degree of hydration-based description of mechanical properties of early age concrete. *Materials and Structures*, 29:335–344, 1996.

Dolado J.S. and van Breugel K. Recent advances in modeling for cementitious materials. *Cement and Concrete Res*, 41(7):711 – 726, 2011.

EN-197-1. *Cement - Composition, specification and conformity criteria - Part 1: Common cements*. CEN - European Committee for Standardization, 2011.

Faria R., Azenha M., and Figueiras J.A. Modelling of concrete at early ages: Application to an externally restrained slab. *Cement and Concrete Composites*, 28(6):572 – 585, 2006.

Hattel J. and Thorborg J. A numerical model for predicting the thermomechanical conditions during hydration of early-age concrete. *Applied Mathematical Modelling*, 27(1):1 – 26, 2003.

Jennings H.M. and Bullard J.W. From electrons to infrastructure: Engineering concrete from the bottom up. *Cement and Concrete Res*, 41(7):727 – 735, 2011.

Kada-Benameur H., Wirquin E., and Duthoit B. Determination of apparent activation energy of concrete by isothermal calorimetry. *Cement and Concrete Research*, 30(2):301 – 305, 2000.

Koenders E. *Simulation of Volume Changes in Hardening Cement-Based Materials*. Ph.D. Thesis, Delft University of Technology, Delft (Netherland), 171 pages., 1997.

Koenders E. *Mix Design for Venice Barriers*. Report Nr. 15.5-05-08, Confidential communication - Delft University of Technology (The Netherlands), 2005.

Lokhorst S. *Deformation behavior of concrete influenced by hydration related changes of the microstructure*. Internal Report, The Netherlands: Delft University Press, 1999.

Martinelli E., Koenders E., and Caggiano A. *A numerical recipe for modelling hydration and heat flow in hardening concrete*. Proposed for publication on Cement and Concrete Composites, 2012.

Midas-IT-User-Manual. *On-line user's manual of Midas NFX*. Research and Development Institute of Midas IT, 2010.

Narasimhan T. Fourier's heat conduction equation: history, influence, and connections. *Reviews of Geophysics*, 37(1):151 – 172, 1999.

Ortiz J., Aguado A., Agullo L., and Garcia T. Influence of environmental temperatures on the concrete compressive strength: Simulation of hot and cold weather conditions. *Cement and Concrete Res*, 35(10):1970 – 1979, 2005.

Pepe M., Koenders E., Caggiano A., Lima C., and Martinelli E. *Sui Processi di Idratazione e le Loro Conseguenze Sulle ProprietÃ Meccaniche Di Calcestruzzi con Componenti Riciclati*. Proceedings of 19 CONGRESSO C.T.E., BOLOGNA, 8-10 Novembre 2012, 2012.

Ulm F. and Coussy O. Modelling of thermo-chemo-mechanical couplings of concrete at early ages. *ASCE J Eng Mech*, 121(7):785 – 794, 1995.

van Breugel K. *Simulation of hydration and formation of structure in hardening cement-based materials*. Delft University Press, The Netherlands, 1991.

van Breugel K. *Concrete structures under temperature and shrinkage deformations*. Lecture notes CT5120, TU Delft - Delft University of Technology (The Netherlands), 2004.